Viscoelasticity of Thin Adhesive Layers as a Function of Cure and Service Temperature Measured by a Novel Technique

R. E. CHALLIS,* R. P. COCKER, A. K. HOLMES, and T. ALPER

Ultrasonics and Digital Signal Processing Laboratory, University of Keele, Staffordshire, ST5 5BG United Kingdom

SYNOPSIS

This article presents a novel short-pulse ultrasonic technique for measuring the relaxing planewave modulus in realistically thin films of adhesive polymer over wide-frequency bandwidths (1 MHz to between 30 and 100 MHz). On-line computational methods are used to correct for known system distortions, for the estimation of absorption, planewave phase velocity, and complex planewave modulus, all as functions of frequency. Where appropriate it is also possible to fit models of relaxation processes to the measured data. Detailed results are shown for nine structural adhesives designed principally for automotive applications. The changes that occur during cure, as a result of extended cure, and with variation in service temperature are demonstrated. This work concludes that the method provides convenient measures of engineering properties, provides the means to study the effects of cure and service conditions, and provides reliable measures of ultrasonic propagation parameters that can be used to investigate the testability of adhered structures by ultrasonic means.

INTRODUCTION

The ability to design and manufacture adhered structural components that have predictable properties and good durability depends very much on adequate knowledge of the mechanical properties of the adhesive polymer and the stability of these under in-service conditions. It is obvious to state that these properties depend on the physicochemical formulation of the adhesive, and frequently, the cure temperature cycle, and the thermal conduction properties of the adhesive and of its immediate environment. There is no simple method to assess nondestructively whether an adhesive material has cured to within a defined band of property values or whether its initial chemical formulation was correct. Most nondestructive tests of adhesive materials and adhesive joints can only give very crude evidence as to whether all is well with the polymer or not. Mechanical or ultrasonic tests are particularly relevant because they give a measure of elasticity, a property of structural importance, and because they could, in principle, be used to identify defects.

A large number of authors have published methods and results describing the application of ultrasonic techniques to polymers, and a full review is beyond the scope of this article. The methods generally divide into those aimed at measuring ultrasonic wave attenuation and those aimed at measuring ultrasonic wave propagation velocity.[1-10] Most techniques are based on near-planewave propagation, although some incorporate shear wave measurements. A further division between techniques groups those in which measurements are made simultaneously over wide-frequency bandwidths and those in which measurements are made at only one, or a few, spot frequencies. Clearly the wider the bandwidth available for measurement the more complete the characterization of the polymer; conversely, spot frequency methods give only limited characterization of polymer properties, particularly loss mechanisms. If measurements of both attenuation and wave propagation velocity are made si-

* To whom correspondence should be addressed.

Journal of Applied Polymer Science, Vol. 44, 65–81 (1992)
 CCC 0021-8995/92/010065-17$04.00

multaneously over wide-frequency bandwidths, then it is possible to derive, in addition, the frequency dependence of the real and imaginary parts of the material elastic modulus, giving a detailed picture of the viscoelasticity of the material. Further advantage is to be gained if the methods can be applied to relatively thin polymer films, less than 1 mm say. The reason for this is that it is often difficult to cast an ingot of adhesive that is of a suitable size and shape for mechanical and ultrasonic testing. This is because many cure reactions are strongly exothermic, causing the polymer to carbonize if all parts of its bulk are not in good thermal contact with an adequately conducting substrate.

In this article we present a method that is applicable to thin adhesive samples and that provides for wide bandwidth measurement of wave attenuation, velocity, and complex modulus. It is based on the reverberation of a short acoustic pulse in a thin layer of adhesive (50 to 200 μm) and provides a measurement bandwidth from 1 MHz to an upper limit that is between 30 and 100 MHz depending on the acoustic losses in the polymer. The information provided by the method is in the form of real and imaginary parts of the planewave modulus ($K + 4G/3$), as continuous functions of frequency over the stated range. Since many adhesives exhibit relaxation in their mechanical properties over this frequency range, we have incorporated into the method a least-mean-square (LMS) algorithm that will estimate relaxation frequency and relaxation strength from the measured data for one or more parallel loss processes. The instrument can be used to study the cure process, the effects of miscure, and the effects of service temperature change. In the sections that follow we outline the technique and present typical experimental results.

THE MEASUREMENT METHOD

The method is based on the test cell shown in Figure 1(a). The adhesive to be tested is formed into a bond between two float glass blocks separated by cylindrical wire spacers of known thickness. Ultrasonic transducers are placed in coaxial alignment on either side of the bonded blocks, and coupled to them by means of compressible aluminum foil layers that also act as electromagnetic screens between the two sides of the cell. One transducer is used as a transmitter and the other as a receiver; both operate in what is known as the acoustically thick mode[11,12] and exhibit operating bandwidths that are much greater than would follow from the simple damped half-wave resonance used in conventional pulsed ultrasound systems (discussed later). The two transducers are connected to electronic driver and receiver circuits, which are modules in the computer-controlled system illustrated in Figure 1(b). The host computer is used to synchronize the operation of the transmission and reception electronics and to carry out data processing tasks. In the present arrangement the computer is a PDP 11/23 machine (Digital Equipment Corporation), but a more modern personal computer equipped with appropriate interfaces would serve just as well. Binary signals from the computer are used to trigger a low-voltage pulse generator (C0), trigger the sampling oscilloscope (C1), and enable a high-voltage pulse circuit (C2) that is triggered by the low-voltage pulse generator. The high-voltage pulse circuit excites the transmitter transducer with a short pulse of 160 V amplitude, with rise and fall times of 0.7 ns and width 5 ns. The interval between excitations is 100 ms. A near-replica of this pulse is transmitted as an edge-diffracted planewave (discussed later) through the first glass block, the adhesive layer, the second glass block, and then to the receiver transducer. The receiver transducer is terminated resistively by 2 Ω and feeds an amplifier of 40-dB gain, 150-MHz bandwidth, and with smooth phase response. The amplifier output is fed to a sampling oscilloscope (Tektronix 7613 frame with 7514 plug-in), ready for signal processing on the computer. Transfer of the analogue waveform from the slow-scan output of the oscilloscope to the host computer is achieved by means of a conventional successive approximation analogue-to-digital converter (ADC) plugged into the computer backplane; it has a maximum sampling rate of 50 kHz and a resolution of 10 bits. With this arrangement it is possible to achieve an effective sampling rate for repetitive signals at the receiver amplifier of 1 GHz.

On its way through the adhesive layer the short pulse reverberates to and fro in a time interval determined by the layer thickness and the wave propagation velocity in the adhesive polymer; these reverberation times are of the order of 100 ns. The thicknesses of the glass blocks and of the ultrasonic transducer elements are chosen so that reverberation times in these components are much greater than the reverberation time in the adhesive layer. This enables the reverberations in the adhesive to be time-resolved independently of the reverberations in the glass blocks and the transducers. Typical reverberations from within the adhesive layer are shown in Figure 2. The principle by which viscoelastic properties are calculated is that successive

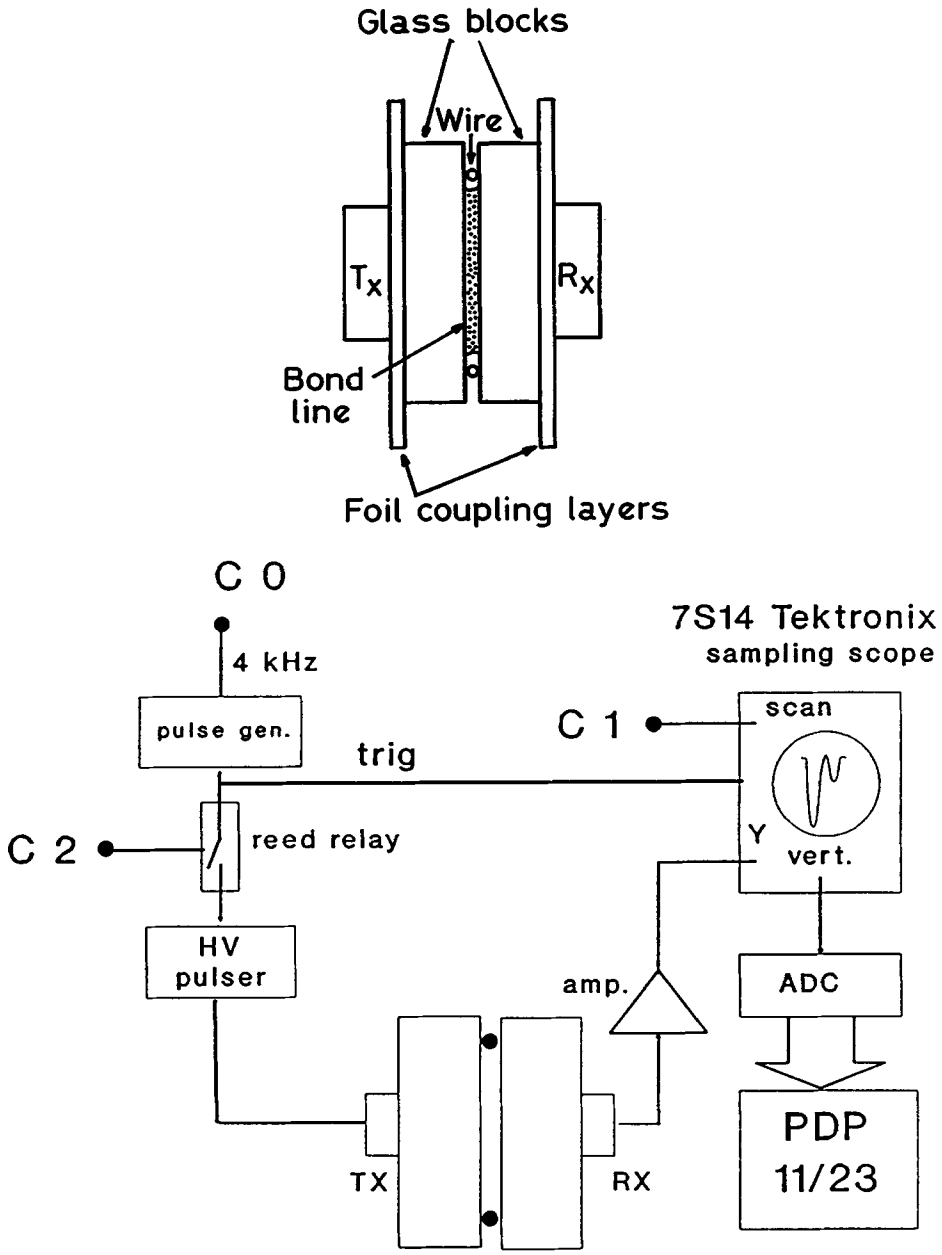

Figure 1 (a) The test cell and (b) diagram of the whole system. The test cell is connected to a high-voltage pulse transmitter and on the receiving side to a wide bandwidth linear amplifier and sampling oscilloscope. The slow-scan output from the oscilloscope is digitized and fed to the host computer (PDP 11/23) for processing. The computer also generates binary signals to synchronize the operation of the pulse generator (C0) and the oscilloscope (C1), and to enable the high-voltage pulse generator (C2).

reverberations will have made two more transits through the adhesive layer than their immediate predecessors. In Figure 2 the first pulse in the trace will have made a single transit across the bond whereas the second pulse will have made a total of three transits (Fig. 3). The change in shape between the first and second pulses is determined in part by interactions between the propagating ultrasonic pulse and the viscoelastic properties of the materials. The principle of this technique is that the relaxing elastic modulus is calculated as a function of frequency on the basis of a frequency domain comparison of the shapes of successive reverberation pulses. However, before this can be done corrections must

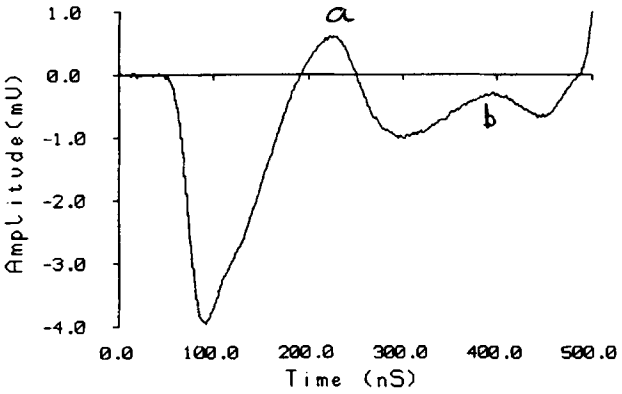

Figure 2 An acoustic reverberation signal from a 170-μm-thick layer of Evode M23 adhesive showing the wake component due to diffraction effects, marked "a," and the exponential rise due to transducer insertion, marked "b."

be made for the effects of the transducer properties and for acoustic field diffraction phenomena, which result from the fact that the transducers are bounded (i.e., not of infinite extent). These effects show as a falling baseline in the later regions of the signal and a positive-going wake in the earlier part of the signal (Fig. 2). These corrections and subsequent viscoelasticity calculations are carried out in the host computer; they are described in the following section.

COMPUTATIONS

Correction of Raw Data

It can be shown[12] that the frequency domain insertion effect of a thick piezoelectric transducer device, when expressed as the Laplace transform transfer function, is

$$H(s) = \frac{ks}{s(1 + s\tau_E) - 1/\tau_M} \tag{1}$$

Here s is complex frequency, $\sigma + j\omega$, k is a constant, τ_E is the electrical time constant formed of the device self-capacitance and its source or load resistance, and τ_M is an electromechanical time constant whose value is set by the transducer material properties and the mechanical loads applied to its acoustic faces. It results in a rising exponential term in the transducer response, and it is the cause of the falling tail in the response shown in Figure 2. The mechanism of this rather bizarre effect has been discussed in a previous publication.[13] In the system described here τ_E for both transducers is kept below about 5 ns by choice of source and load resistances and Eq. (1) can be simplified to

$$H(s) = \frac{ks}{s - 1/\tau_M} \tag{2}$$

A filter designed to correct for this effect would have a transfer function of the form

$$C(s) = \frac{1}{H(s)} = \frac{1}{k}\left[1 - \frac{1}{s\tau_M}\right] \tag{3}$$

We have implemented a filter of this form as a discrete time-domain algorithm using conventional digital filter design methods;[14,15] its effect on signals of the form shown in Figure 2 is to remove the falling tail and to *slightly* alter the shape of the reverberating pulses.

The radiation coupling process between the two transducers is such that, for an ideal Dirac function excitation to the transmitter face, the receiver will respond with a signal at its terminals that consists of that Dirac function delayed in time due to the propagation path length, and then followed immediately by a wake component of opposite sign, known as the edge wave or diffracted component. This is the cause of the rising baseline in the early part of the signal shown on Figure 2. Formulations of the effect have been presented by many workers.[16,17] In this method we make a correction to the digitized data in the discrete frequency domain, using methods developed for a related instrument.[12] The result of this and the transducer correction process is to set the train of reverberation pulses on to a flat base line (Fig. 4). This greatly facilitates their separation

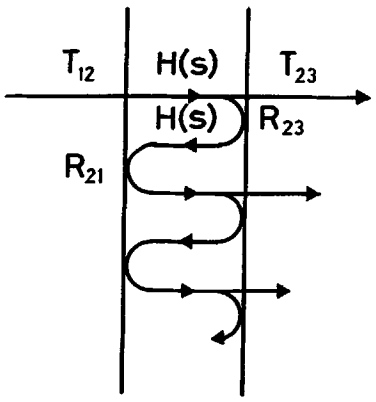

Figure 3 Diagram illustrating the reverberative propagation path within the adhesive.

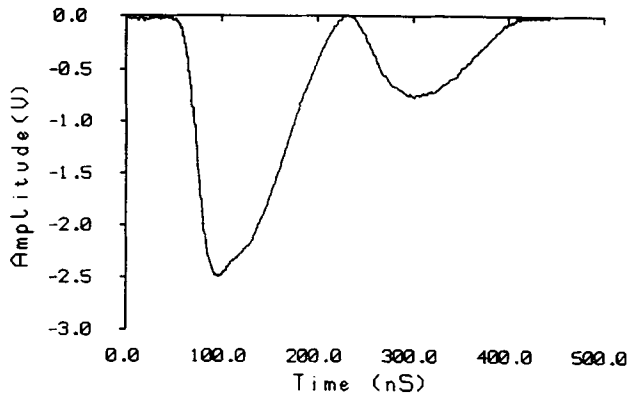

Figure 4 The data of Figure 2 after correction for system effects.

as two distinct time-domain events, which is required for calculations of the planewave modulus.

Calculation of the Planewave Modulus

We define the planewave modulus as a complex frequency dependent quantity:

$$M(\omega) = M_R(\omega) + jM_I(\omega) \tag{4}$$

where ω is a real radian frequency, j is the operator $(-1)^{1/2}$, and subscripts R and I denote real and imaginary parts. For a planewave traveling in the positive x direction in a medium of modulus $M(\omega)$ and density ρ, the wave pressure amplitude at x compared to that at $x = 0$ is, in the frequency domain,

$$P(x, \omega) = P(0, \omega)e^{-\alpha(\omega)x}e^{-j\omega x/c(\omega)} \tag{5}$$

Here $\alpha(\omega)$ is the planewave amplitude absorption coefficient, generally a function of frequency, and $c(\omega)$ is the phase velocity, also a function of frequency in the general case. After much tedious algebra[18] $M(\omega)$ can be related to $\alpha(\omega)$ and $c(\omega)$ as follows:

$$M_R(\omega) = \rho c^2(\omega) \frac{1 - \alpha^2(\omega)c^2(\omega)/\omega^2}{[1 + \alpha^2(\omega)c^2(\omega)/\omega^2]^2} \tag{6a}$$

$$M_I(\omega) = \rho c^2(\omega) \frac{2c^3(\omega)\alpha(\omega)/\omega}{[1 + \alpha^2(\omega)c^2(\omega)/\omega^2]^2} \tag{6b}$$

In our computations we first calculate $\alpha(\omega)$ and $c(\omega)$ from the precorrected data and then we calculate $M(\omega)$ from Eqs. (6a) and (6b).

Calculation of $\alpha(\omega)$ and $c(\omega)$

Absorption coefficient and phase velocity are calculated from the shape change between the first two successive reverberations in Figure 4. A number of different computational techniques have been tried and will be presented in a later publication; only the simplest method will be described here. The first task is to estimate the low-frequency planewave velocity as follows: The positions on the time axis that correspond to the centers of area of the two pulses are calculated from the digitized data using the method of moments. If these times are T_A and T_B, respectively, and if the bond thickness is X, then the low-frequency velocity is given by

$$c_0 = \frac{2X}{T_A - T_B} \tag{7}$$

The two digitized pulses A and B are then separately shifted leftwards in time until both of their centers of area correspond to the notational zero of time for the digitized data. The fast Fourier transform (FFT) of each is calculated as a complex function of frequency. These have modulus spectra $|A(\omega)|$ and $|B(\omega)|$ and phase spectra $\theta_A(\omega)$ and $\theta_B(\omega)$, respectively. The absorption coefficient is calculated from the moduli of the raw frequency spectra, thus

$$\alpha(\omega) = \frac{1}{2X} \ln \frac{|A(\omega)|}{|B(\omega)|} \cdot \frac{B(0)}{A(0)} \tag{8}$$

The term $B(0)/A(0)$ is included to eliminate the effect of the internal reflection coefficients between the adhesive and the glass substrate, both of which are assumed to be independent of frequency. Phase velocity is calculated from the two phase spectra as follows:

Before leftward shifting of the digitized data a frequency component in pulse A would, in traversing the adhesive once only, be phase shifted:

$$\Delta\theta_A = -\omega X/c(\omega) \tag{9a}$$

similarly a frequency component in pulse B would be shifted three times this amount:

$$\Delta\theta_B = -3\omega X/c(\omega) \tag{9b}$$

Now, because of the leftward time shifts applied to the digitized data, the computed shifts will be

$$\theta_A = \omega T_A - \omega X/c(\omega) \tag{10a}$$

$$\theta_B = \omega T_B - 3\omega X/c(\omega) \tag{10b}$$

The difference between these two is

$$\Delta\theta = \theta_B - \theta_A = \omega(T_B - T_A) - 2\omega X/c(\omega) \quad (11)$$

Now substituting from Eq. (7) for $T_B - T_A$ we get

$$\Delta\theta = 2\omega X[1/c_0 - 1/c(\omega)] \quad (12)$$

from which $c(\omega)$ can be calculated as

$$c(\omega) = \frac{c_0}{1 - (\Delta\theta c_0/2\omega X)} \quad (13)$$

This value of $c(\omega)$ and the value of $\alpha(\omega)$ calculated from Eq. (8) are used in the computation of Eq. (6) to calculate the real and imaginary parts of the planewave elastic modulus.

Estimation of Relaxation Parameters

A material that exhibits a single time constant viscoelastic relaxation (Fig. 5) has the complex modulus

$$M(\omega) = M_0 \frac{1 + j\omega\tau_2}{1 + j\omega\tau_1} \quad (14)$$

where M_0 is the low-frequency (real) modulus, and τ_1 and τ_2 are time constants that relate to the viscous and elastic elements in Figure 5 thus

$$\tau_1 = \eta/k_a \quad (15a)$$

$$\tau_2 = \eta(k_a + k_b)/k_a k_b \quad (15b)$$

It is convenient to reexpress Eq. (14) as

$$M(\omega) = M_0 \frac{1 + j\omega a\tau}{1 + j\omega\tau/a} \quad (16a)$$

where

$$a^2 = \tau_2/\tau_1 \quad \text{and} \quad \tau = \sqrt{\tau_1\tau_2} \quad (16b)$$

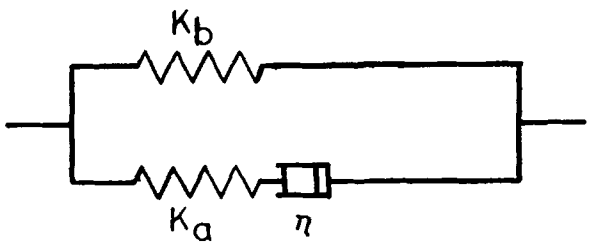

Figure 5 Mechanical model representing a single relaxation process.

The real and imaginary parts of the modulus are

$$M_R = M_0 \frac{1 + \omega^2\tau^2}{1 + \omega^2\tau^2/a^2} \quad (17a)$$

$$M_I = M_0 \frac{\omega\tau(a - 1/a)}{1 + \omega^2\tau^2/a^2} \quad (17b)$$

If this modulus is incorporated into the one-dimensional planewave equation, then the phase velocity becomes, for small a,

$$\frac{c^2}{c_0^2} = \frac{1 + a^2\omega^2\tau^2}{1 + \omega^2\tau^2} \quad (18)$$

The acoustic absorption per wavelength is given by

$$\alpha\lambda = \pi(a - 1/a) \frac{\omega\tau}{1 + \omega^2\tau^2} \quad (19)$$

The relaxation parameters to be estimated are the strength a and the relaxation time constant τ, or the corresponding relaxation frequency $f_r = 1/2\pi\tau$. In our system, functions of the form of Eqs. (18) and/or (19) can be fitted to measured data using Marquardt's LMS algorithm.[20] We have organized our signal processing software to fit any arbitrary number of relaxation processes, although for the purposes of the current work we have constrained its operation to a single relaxation. It should be noted that there are alternative formulations[19] to relaxation phenomena in which the strength parameter ϵ is given by

$$\epsilon = 1 - 1/a^2 \quad (20a)$$

or

$$a = (1 - \epsilon)^{-1/2} \quad (20b)$$

These yield the following expressions for phase velocity and absorption per wavelength:

$$\frac{c^2}{c_0^2} = 1 + \frac{\epsilon}{1 - \epsilon} \cdot \frac{\omega^2\tau^2}{1 + \omega^2\tau^2} \quad (21)$$

and

$$\alpha\lambda = \pi \frac{\epsilon}{\sqrt{1 - \epsilon}} \cdot \frac{\omega\tau}{1 + \omega^2\tau^2} \quad (22)$$

EXPERIMENTAL MEASUREMENTS

Table I lists the nine different adhesives that were employed in this study; all except one (RS epoxy) were designed principally for automotive applications. For each adhesive type, batches of five bonds were formed between glass blocks as described earlier and cured in a temperature-controlled oven, following the manufacturer's temperature cycle recommendations. During cure the bonds were maintained in compression by means of a 2-kg weight resting on the glass block–adhesive–glass block test piece. The test bond thicknesses were 120, 150, or 170 μm; the uniformity of thickness was better than ± 3 μm across the bond, and the tolerance of mean thickness was better than ± 5 μm for all bonds tested. A small sample of each adhesive was cured separately, and its density measured by the density bottle method. In order to check against the possibility that acoustic scattering could significantly affect our wave propagation results, we studied a section of free adhesive surface with the scanning electron microscope (SEM) at either X800 or X8000 magnification in order to estimate the size of any inhomogeneities such as filler particles or bubbles. All inclusions were at least two orders of magnitude smaller than the wavelengths contained in the propagated ultrasonic pulse. One bond formed of cold-curing epoxy (RS epoxy) was studied throughout its cure cycle, and another was subjected to limited temperature variation in the range 20–60°C. A third sample (M23, Evode Ltd.) was subjected to an extended cure cycle: 60 min at 200°C instead of the normal cure of 30 min at 180°C. The results for all these experiments are described in the following sections.

Typical Wide Bandwidth Data

Figure 6(a) shows, for Kelseal adhesive, typical primary results as functions of frequency—absorption per wavelength, phase velocity, and the real and imaginary parts of the planewave modulus. We note variability within a batch of five bonds and suggest that this is due to uneven temperatures and cooling paths in our curing oven. The results show typical relaxation behavior as far as we can tell within the 40-MHz bandwidth. Degraded signal-to-noise ratio prevented our obtaining meaningful results above this frequency. The maximum value of the imaginary modulus was around 3×10^8. This value was close to half the change in the real modulus between its low-frequency and high-frequency values. This relationship would be expected from a single relaxation process of the type shown in Figure 5. Figure 6(b) gives a comparison of the averaged results for each of the adhesives studied.

Relaxation Parameter Fits

For a cold curing adhesive (RS epoxy) the sets of the five $\alpha\lambda$ curves and the five phase velocity curves were averaged by simple additions of the five versions of each function. The averaged velocity versus frequency curve is shown as the solid line on the top graph of Figure 7. The averaged absorption per wavelength trace is shown as the solid line on the bottom graph of the same figure. The dotted traces on the two graphs on Figure 7 are the predicted velocity and absorption data, predicted on the basis of a and f_r obtained by fitting Eq. (18) to the raw averaged velocity data. The functions formed of crosses are the velocity and absorption data predicted on

Table I Summary of Adhesives Used

Adhesive	Manufacturer	Generic Type	Cure Cycle	Applications
M23	Evode Ltd.	Elastosol	30 min at 180°C	Automotive
M33	Evode Ltd.	Elastosol	30 min at 180°C	Automotive
Kelseal 16.152	Evode Ltd.	PVC and related copolymers	30 min at 155°C	Automotive
DP70-0127	Evode Ltd.	2 part modified epoxy	24–48 h at 20°C	Industrial/automotive
Teroson	W.R. Grace Ltd.	1 part acrylic	30 min at 155°C	Industrial/automotive
RS high strength epoxy	RS Components Ltd.	2 part epoxy	24 h at 20°C	Industrial/domestic
E5238	Bostik Ltd.	1 part epoxy	30 min at 155°C	Automotive
Araldite 2007	Ciba-Geigy Ltd. (Plastics Division)	1 part epoxy	40 min at 160°C	Automotive/industrial
XB 3131	Ciba-Geigy Ltd. (Plastics Division)	1 part epoxy	30 min at 155°C	Automotive

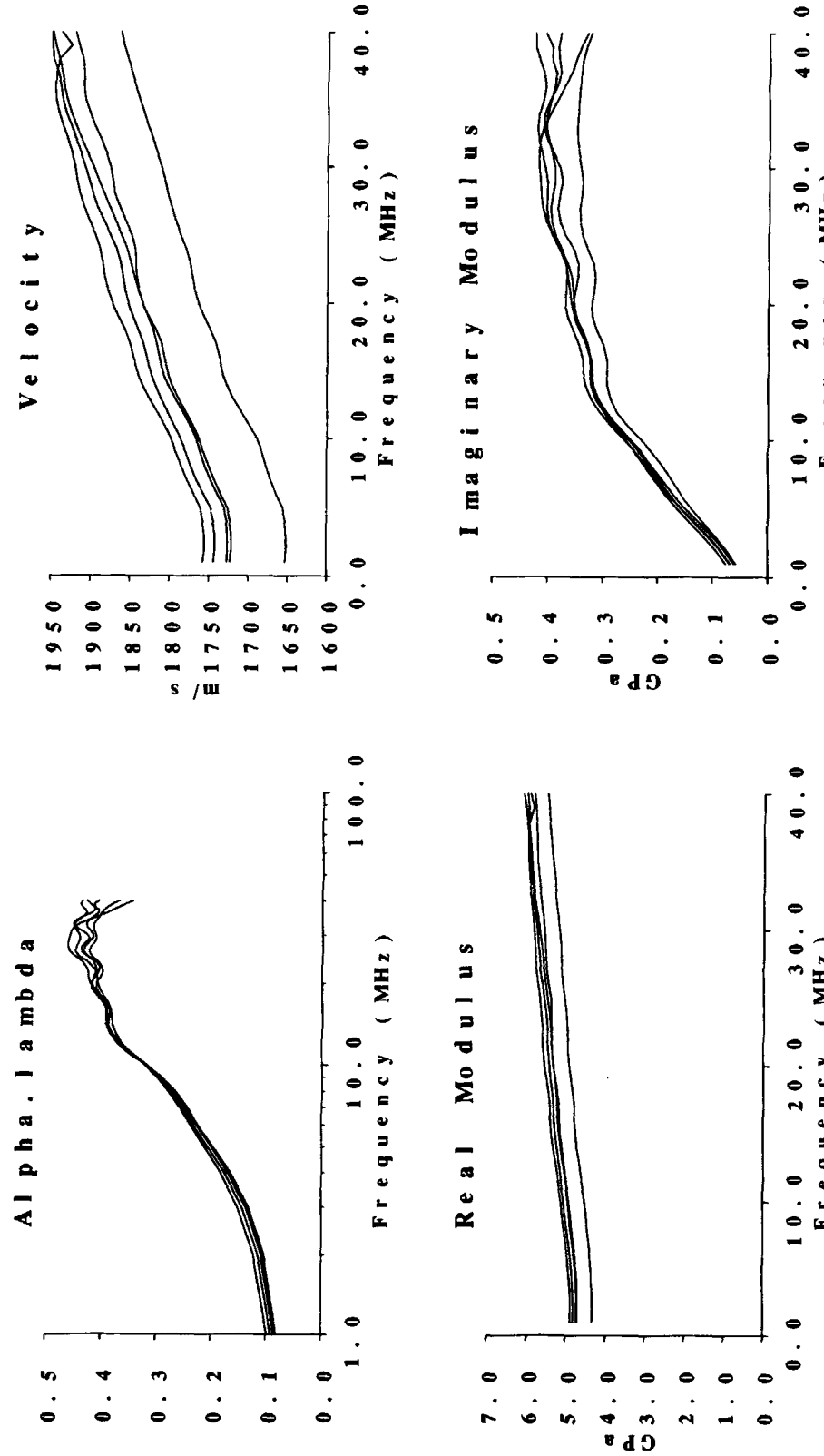

Figure 6(a) Typical wide bandwidth results for Kelseal adhesive. The graphs show absorption per wavelength, phase velocity, real modulus, and imaginary modulus, all as functions of frequency in the range up to 40 MHz. Five curves are shown for each function representing the behavior of the different bonds in a single group of five samples.

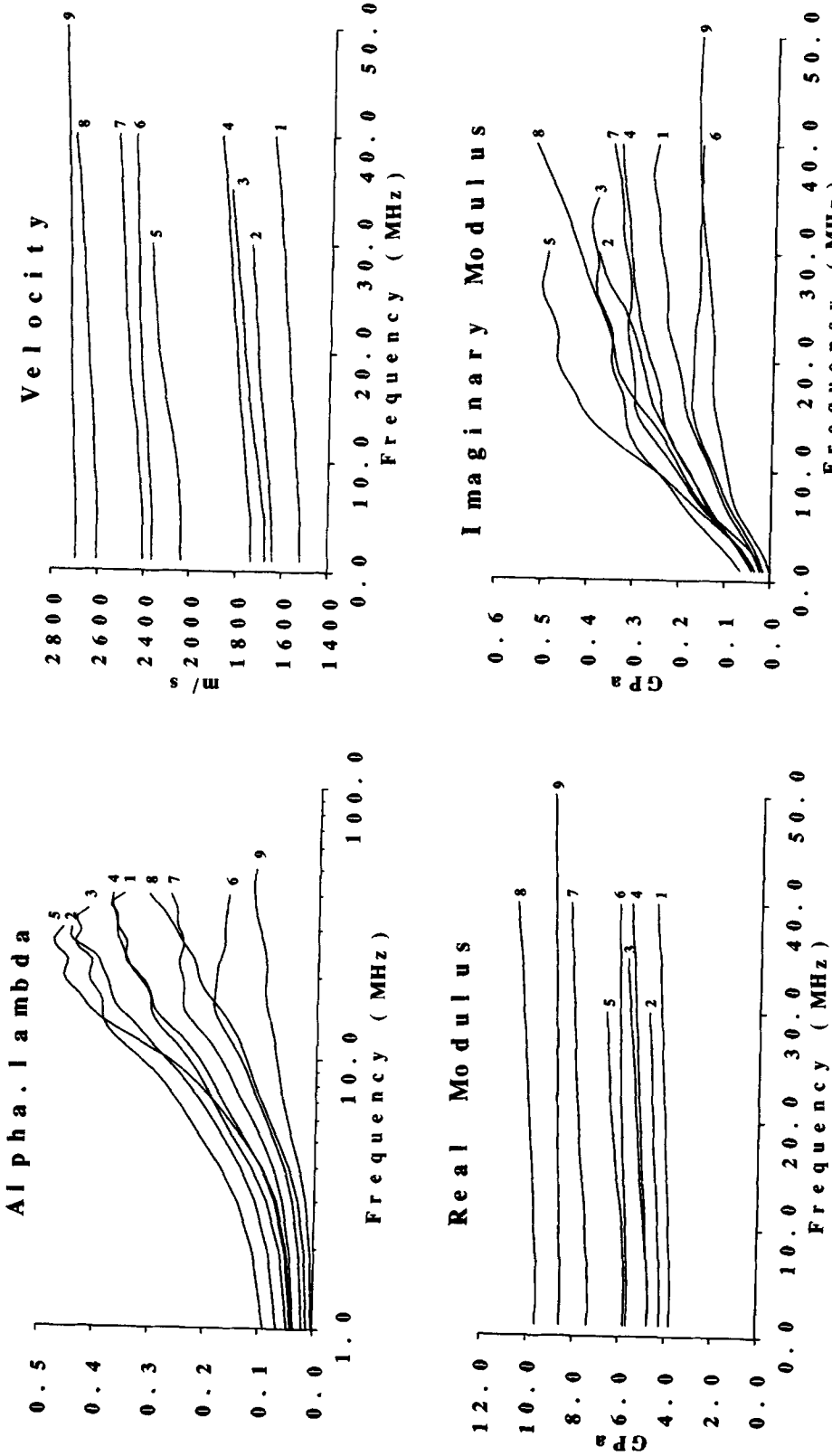

Figure 6(b) Similar data to Figure 6(a), but showing the average of five sample bonds for each of the nine adhesives used in this study. The key to the adhesive types is : 1 = M23, 2 = Teroson, 3 = Kelseal, 4 = M33, 5 = DP70, 6 = RS Epoxy, 7 = E5238, 8 = XB3131, 9 = 2007.

the basis of a and f_r obtained by fitting Eq. (19) to the raw averaged absorption data. We note consistency in these results: Both sets of fitted data agree well with the measured results. Also absorption can be predicted reliably from velocity data and vice versa.

For all of our adhesives we have investigated variability in our fits to relaxation processes and in other basic data; these are described in the next section.

Bond Data and Its Variability

The principal results for all of the eight adhesive types tested are shown on Table II. For each adhesive type we show the mean of five measurements of the low-frequency modulus M_0 and of the low-frequency propagation velocity c_0. There follows the fitted relaxation parameters f_r and a, shown in two groups representing parameters fitted to phase velocity data and parameters fitted to absorption data, respectively. For each parameter a second column gives the standard deviation as an estimate of the variability between the five measurements that contribute to the mean parameter value. A number of comments can be made on these results: First, the low-frequency modulus and the low-frequency velocity values are associated with relatively low standard deviations that give measurement uncertainties in the ranges 1.9–6.4% for modulus and 1.1–2.2% for velocity. The relaxation data is associated with much higher variability as evidenced by higher standard deviation (SD) values in relation to the means. This is to be expected for two reasons: (a) Minor inhomogeneities in the adhesive material are more likely to interact with the higher frequency components in the short acoustic pulse used in our apparatus, due to their dimensions being closer to the wavelengths of those components. (b) The absorption of ultrasound in adhesives increases with frequency, and this brings about worsened signal-to-noise ratio (SNR) in our raw data at high frequencies. The relaxation data fitting procedures are sensitive to the raw data SNR, and increased noise at the receiving transducer maps into increased variability in our derived parameters. The SDs associated with f_r and a fitted from absorption data are generally much smaller than the corresponding SDs for f_r and a fitted from the phase velocity data. The reasons for the better performance of the absorption data fit are twofold: (a) The phase velocity is calculated by means of a phase unwrapping technique that is more sensitive to raw data SNR than is the absorption calculation, and (b) the peak of the absorption curve is more clearly defined than the rather gentle inflexion in the corresponding velocity curve.

Changes during Normal Curve

A bond formed of room temperature curing epoxy was studied over a 4-day cure cycle. Wide bandwidth raw data were captured under computer program control 5 min after the bond was formed, then after

Table II Summary of Basic Data Measured for Adhesives Detailed in Table I[a]

					From Phase Velocity				From Absorption Data			
	M_o (GPa)		C_o (ms^{-1})		f_r (MHz)		a		f_r (MHz)		a	
Adhesive	Mean	SD	Mean	SD	Mean	SD	Mean	SD	Mean	SD	Mean	SD
Teroson	4.16	0.12	1676	25	24.3	6.31	1.127	0.036	28.0	5.84	1.146	0.027
M23	3.76	0.08	1543	16	35.3	3.58	1.155	0.029	28.4	1.11	1.113	0.010
M33	4.72	0.26	1791	48	28.7	3.16	1.129	0.015	28.4	2.59	1.124	0.006
Kelseal	4.64	0.20	1708	36	23.6	1.51	1.162	0.013	23.3	0.68	1.149	0.003
DP70	6.01	0.22	2141	39	36.9	17.19	1.237	0.213	31.5	6.32	1.171	0.034
RS epoxy	5.61	0.24	2289	51	24.3	1.81	1.066	0.006	21.6	0.85	1.060	0.005
E5238	7.30	0.47	2334	75	26.6	0.87	1.092	0.005	26.7	1.85	1.087	0.006
2007	8.54	0.41	2681	44	46.0	17.75	1.050	0.009	38.1	11.11	1.039	0.006
XB3131	9.59	0.47	2571	63	63.3	24.59	1.177	0.099	43.9	9.20	1.095	0.012

[a] For each parameter the columns give the mean calculated for each group of five bonds and the standard deviation of the five values. The tabulated parameters are low-frequency (real) planewave modulus M_o, low-frequency phase velocity C_o, relaxation frequency f_r, and relaxation parameter a, calculated from LMS fits to velocity data and LMS fits to the absorption data.

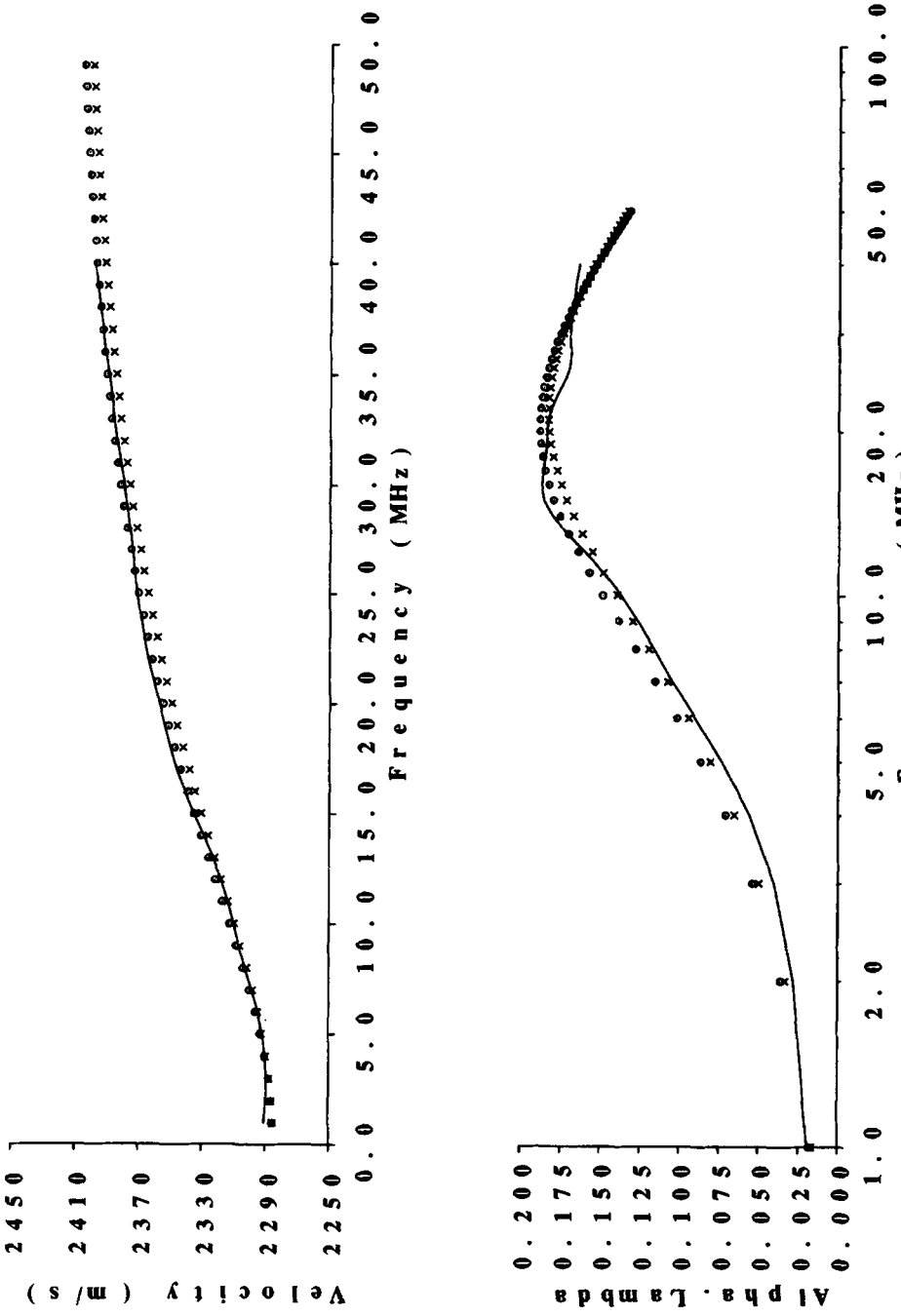

Figure 7 Phase velocity (top) and absorption per wavelength (bottom) for RS epoxy cold curing adhesive as functions of frequency. The solid lines are measured data, the dotted lines are predictions from LMS fits of a single relaxation process to the measured velocity data, and the crossed lines are predictions from LMS fits of a single relaxation process to the measured absorption data.

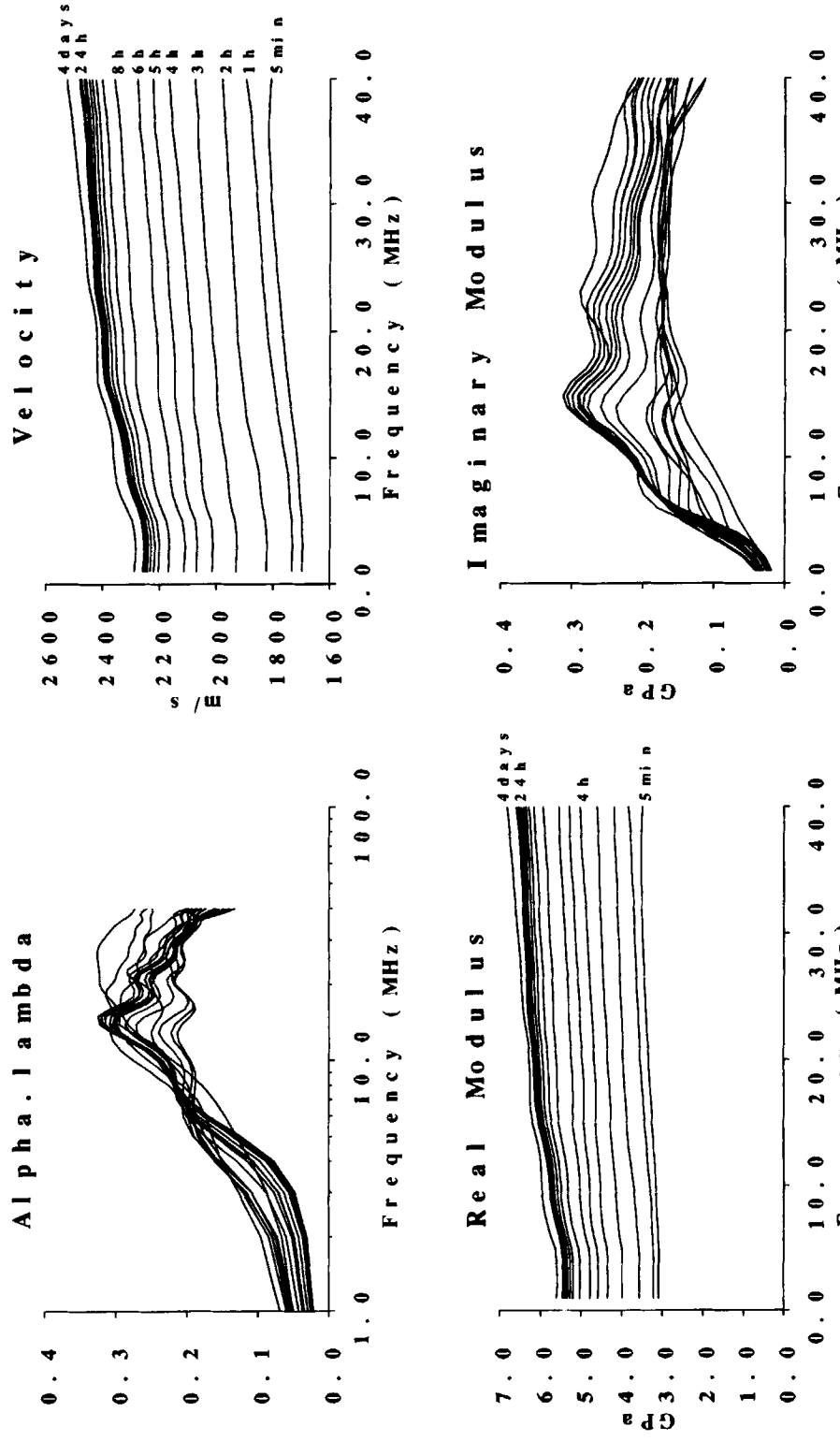

Figure 8 Absorption per wavelength, phase velocity, and complex modulus data at different times during cure for cold curing RS epoxy. Measurements were made at 5 min after bond formation, then at one hourly intervals up to 6 h, and then at two hourly intervals up to 24 h. A final isolated measurement was made at 4 days.

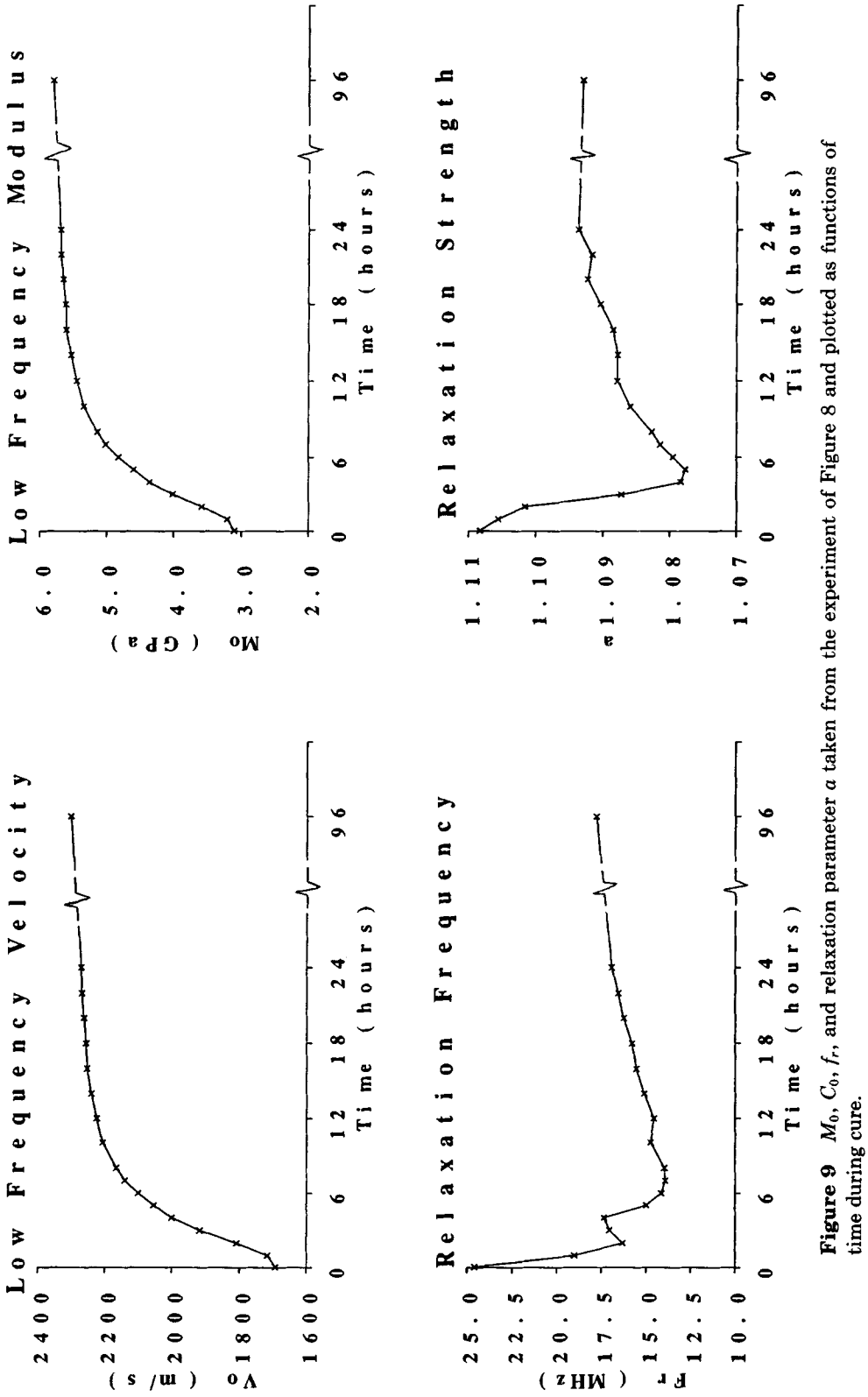

Figure 9 M_0, C_0, f_r, and relaxation parameter α taken from the experiment of Figure 8 and plotted as functions of time during cure.

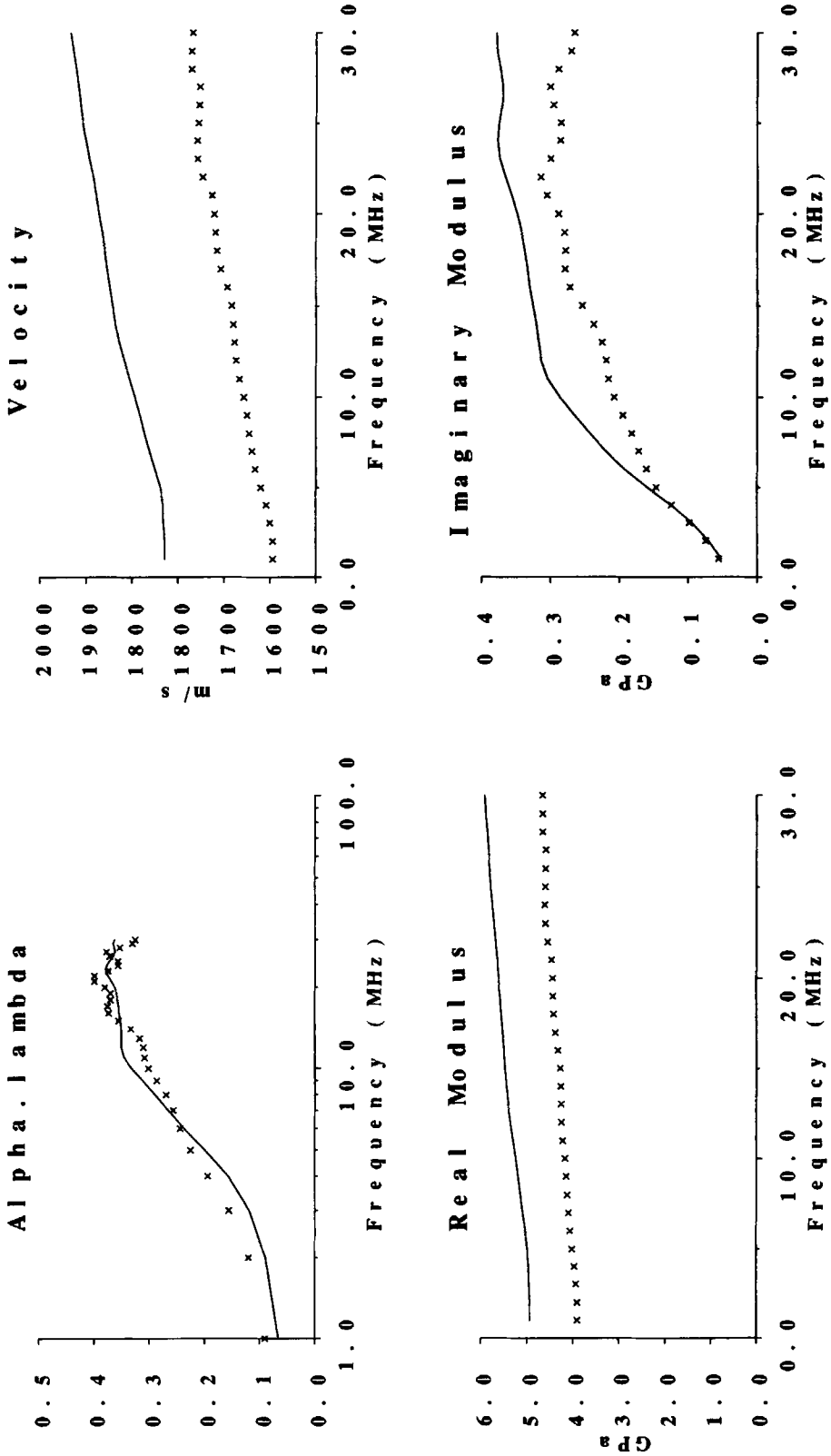

Figure 10 Absorption, phase velocity and complex modulus data to illustrate the effect of excess curing on M23 elastosol adhesive (Evode Ltd.). The crossed lines give results for the manufacturer's recommended cure cycle of 30 min at 180°C while the solid line shows the results for cure at 200°C for 60 min.

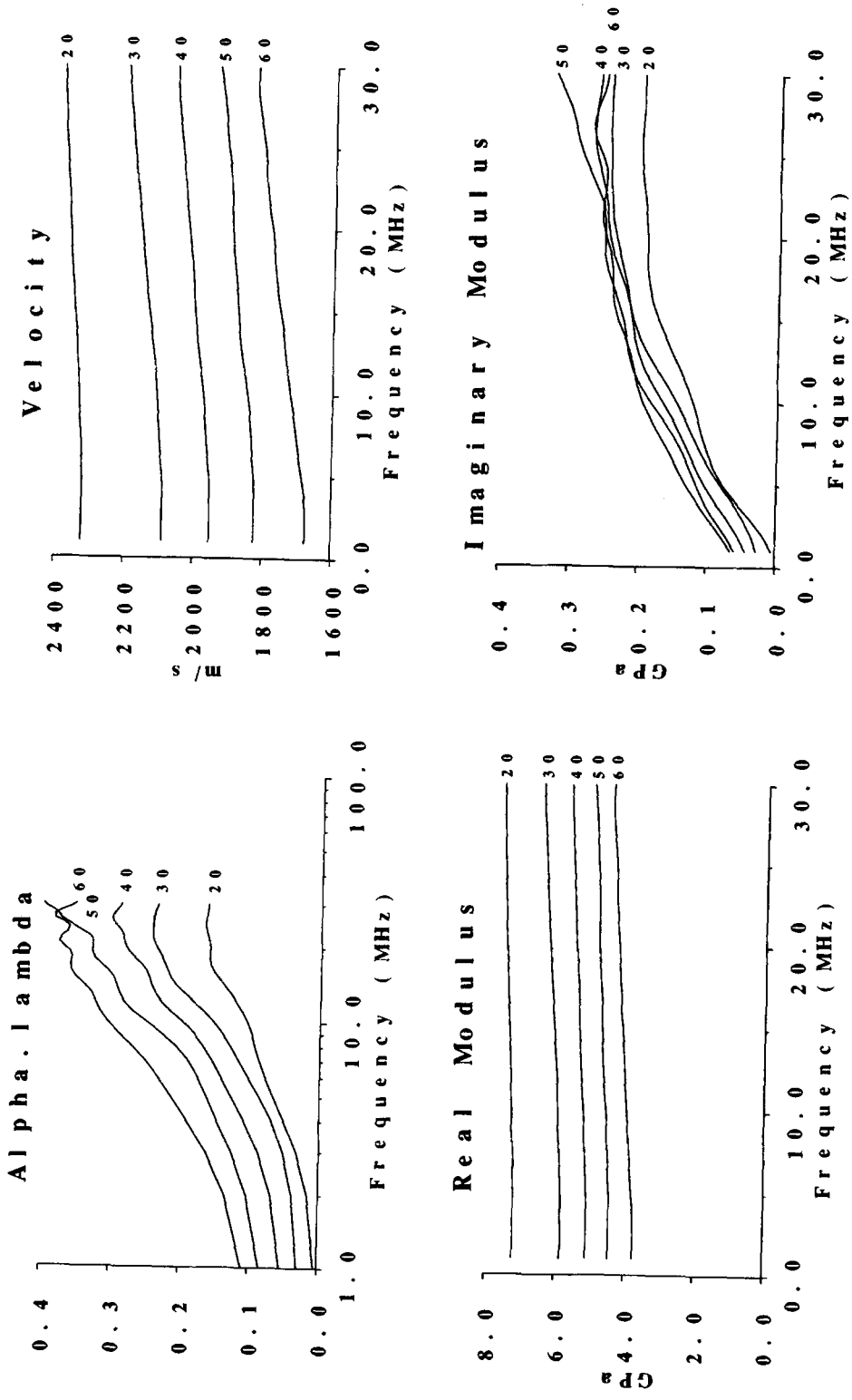

Figure 11 Absorption, phase velocity, and complex modulus data for a single bond of E5238 epoxy (Bostik Ltd.) showing the effect of increasing the temperature of the cured bond in the range 20–60°C.

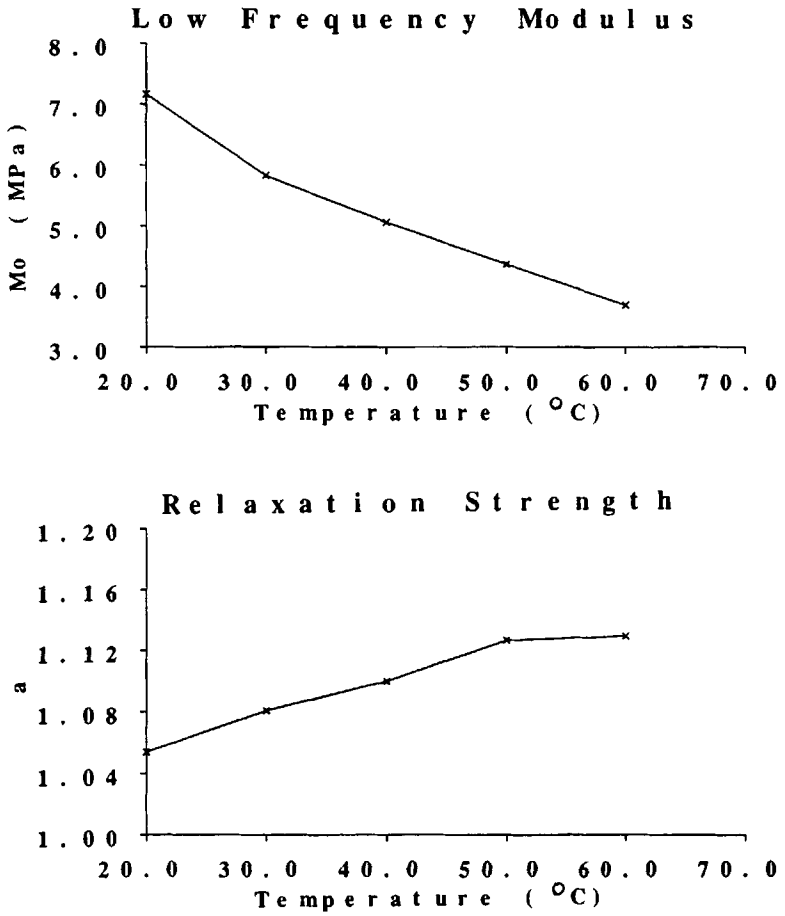

Figure 12 Low-frequency value of the real modulus M_0 and the relaxation parameter a plotted versus temperature for the experiment of Figure 11.

1 h, and thereafter at hourly intervals up to 6 h, and then two hourly intervals up to 24 h. A single final measurement was then made at 4 days. The wide bandwidth data are shown in Figure 8. We have made only minimal attempts to minimize the effects of poor SNR in this experiment, and this accounts for the rather variant form of the imaginary modulus and absorption data. We have plotted the principal changes that take place during cure in Figure 9, which shows the variation of M_0, c_0, f_r, and a as functions of time during cure. The hardening of the material is evidenced by the gradual monotonic increase in low-frequency modulus and low-frequency phase velocity with time. The fitted relaxation parameters are interesting in that both center frequency and strength begin at relatively high values, fall to a minimum at around 8 h, and then increase again to reach final values that are between the minimum and the initial high value. At the present time we do not offer an explanation for this phenomenon.

Effect of Extended Cure

Figure 10 shows the basic wide bandwidth results for bonds formed of M23 elastosol adhesive (Evode Ltd.) when subjected to different cure cycles. The crossed lines show data for the normal manufacturers recommended cure cycle of 30 min at 180°C while the solid lines show what happens when the adhesive is cured for 60 min at 200°C. The principal result is an increase in the real modulus by about 27% across the whole measurement frequency range. The absorption per wavelength curve did not change appreciably, from which we conclude that vibrational states in the polymers that contribute to absorption are not affected by extended cure and, indeed, are not greatly changed during cure either, as evidenced by the results of the last section.

The Effect of Service Temperature

A single bond from the E5238 epoxy series (Bostik Ltd.) was tested in the temperature range 20–60°C

and the results are shown in Figure 11. We note that the real modulus falls rapidly with rising temperature as would be expected as the adhesive softens. The imaginary modulus tends to rise with increasing temperature as does the relaxation strength as evidenced by the height of the $\alpha\lambda$ curve. The relaxation frequency stays roughly constant over the temperature range studied. The principal changes with temperature as shown in Figure 12.

DISCUSSION

This article has presented a novel acoustic technique by which the planewave modulus can be estimated in adhesive films in terms of its real and imaginary parts expressed as functions of frequency in bandwidths up to between 30 and 100 MHz, depending on adhesive type. Where relaxation processes are present, estimates of relaxation frequency and strength are made as part of the modulus computation. The method is relatively cheap and rapid in operation. It can be left under computer control for extended periods and used to study cure processes and the effects of in-service temperature variation, as these evidence themselves in the measured viscoelastic properties.

In the area of nondestructive testing (NDT) of adhered structures, there are many uncertainties associated with the detectability of small flaws due to the fact that high frequencies (i.e., short wavelengths) are required, and these are heavily attenuated in most adhesive polymers. The method presented here provides reliable estimates of acoustic planewave absorption coefficient and propagation velocity as functions of frequency and is currently being employed as an aid to developing quantitative measures of flaw detectability.

CONCLUSION

We conclude that our instrument and associated computational methods have three important areas of application: (1) They provide a means to measure viscoelastic parameters in realistically thin films of adhesive. (2) They provide a simple basis for investigating the cure process, the effects of service conditions, and, potentially, aging. (3) They provide reliable measures of absorption and velocity dispersion that can be used to investigate the testability of adhered structures by ultrasonic means.

The authors acknowledge with thanks the support of the UK Science and Engineering Research Council and the Ford Motor Company.

REFERENCES

1. A. G. Dietz, E. A. Hauser, F. J. McGarry, and G. A. Sofer, *Ind. Eng. Chem.*, **48,** 75 (1956).
2. B. Hartman and J. Jarzynski, *J. Appl. Phys.*, **43,**
3. J. W. Nanziato and H. J. Sutherland, *J. Appl. Phys.*, **44,** 184–187 (1973).
4. J. H. Speake, R. G. C. Arridge, and G. J. Curtis, *J. Phys. D., Appl. Phys.*, **7,** 412–424 (1974).
5. I. Perepechko, *Acoustic Methods of Investigating Polymers,* Mir Publishers, Moscow, 1975.
6. A. M. Lindrose, *Exper. Mech.*, **18,** 227–232 (1978).
7. K. Adachi, G. Harrison, J. Lamb, A. M. North, and R. A. Pethrick, *Polymer,* **8,** 1032–1039 (1981).
8. R. A. Kline, Materials Characterisation Using an Ultrasonic Spectroscopy Technique; ASNT Meeting, Dallas, in *Qualtest II,* **23,** 1–7 (1983).
9. W. N. Reynolds, L. P. Scudder, and H. Pressman, *Polym. Testing,* **6,** 325–336 (1986).
10. J. N. Prassianakis, *J. App. Polym. Sci.*, **39,** 2031–2041 (1990).
11. R. G. Peterson and M. Rosen, *J. Acoust. Soc. Am.*, **41,** 336–341 (1966).
12. R. E. Challis, A. K. Holmes, J. A. Harrison, and R. P. Cocker, *Ultrasonics,* **28,** 5–15 (1990).
13. R. E. Challis and J. A. Harrison, *J. Acoust. Soc. Am.*, **74,** 1673–1680 (1983).
14. R. E. Challis and R. I. Kitney, *J. Biomed. Eng.*, **4,** 267–278 (1982).
15. T. J. Terrell, *Introduction to Digital Filters,* MacMillan, London, 1980.
16. T. L. Rhyne, *J. Acoust. Soc. Am.*, **61,** 318–324 (1977).
17. J. A. Harrison, G. N. Cook-Martin, and R. E. Challis, *J. Acoust. Soc. Am.*, **76,** 1009–1022 (1984).
18. H. J. McSkimin, "Ultrasonic Methods for Measuring the Mechanical Properties of Liquids and Solids," in *Physical Acoustics,* Vol 1A, W. P. Mason, Ed., Academic Press, New York, 1964.
19. H. J. Bauer, "Phenomenological Theory of the Relaxation Phenomena in Gases," in *Physical Acoustics Part 2A,* W. P. Mason, Ed., Academic Press, New York, 1965.
20. D. W. Marquardt, *J. Soc. Indust. Appl. Math.*, **11**(2) (1963).

Received December 21, 1990
Accepted February 11, 1991